Cell, Vol. 95, 951–961, December 23, 1998, Copyright ©1998 by Cell Press

Crystal Structure of the Human High-Affinity IgE Receptor

Scott C. Garman,* Jean-Pierre Kinet,† and Theodore S. Jardetzky*‡

*Department of Biochemistry, Molecular Biology, and Cell Biology
Northwestern University
Evanston, Illinois 60208

†Laboratory of Molecular Allergy and Immunology
Harvard Medical School
Boston, Massachusetts 02215

Summary

Allergic responses result from the activation of mast cells by the human high-affinity IgE receptor. IgE-mediated allergic reactions may develop to a variety of environmental compounds, but the initiation of a response requires the binding of IgE to its high-affinity receptor. We have solved the X-ray crystal structure of the antibody-binding domains of the human IgE receptor at 2.4 Å resolution. The structure reveals a highly bent arrangement of immunoglobulin domains that form an extended convex surface of interaction with IgE. A prominent loop that confers specificity for IgE molecules extends from the receptor surface near an unusual arrangement of four exposed tryptophans. The crystal structure of the IgE receptor provides a foundation for the development of new therapeutic approaches to allergy treatment.

Introduction

The high-affinity IgE Fc receptor (FcεRI) triggers the activation of effector cells, leading to allergic reactions and anaphylactic shock. Human FcεRI exists in two forms, as an αβγ2 tetramer or an αγ2 trimer. The α subunit is involved in IgE binding, and the β and γ subunits are the signal transduction modules. Genetic evidence for a prominent role of FcεRI in mediating allergic reactions has been provided by various studies. Mice lacking the gene for the receptor α chain are unable to mount IgE-mediated anaphylaxis (Dombrowicz et al., 1993), and the β subunit of FcεRI has been associated with asthma in genetic studies (Shirakawa et al., 1994; Hill et al., 1995; Hill and Cookson, 1996; Kim et al., 1998; Mao et al., 1998).

A significant fraction of the population (~20%) is affected by allergies (Sutton and Gould, 1993), and this century has seen a substantial increase in asthma, which now accounts for approximately one-third of US pediatric emergency room visits (Cookson and Moffatt, 1997). Since IgE binding to FcεRI is an obligatory step in the initiation of reactions to different allergens, therapeutic strategies aimed at inhibiting IgE/FcεRI interactions could provide a single treatment for these diseases. In this regard, knowledge of the three-dimensional structure of FcεRI may guide the design of new molecules and approaches to treating allergy and asthma.

FcεRI belongs to a family of antibody Fc receptors (FcRs) that play an important role in the immune response by coupling the specificity of secreted antibodies to a variety of cells of the immune system (Sutton and Gould, 1993; Metzger, 1994; Ravetch, 1994; Daeron, 1997). FcR-initiated reactions of the immune system are important in normal immunity, as well as in allergies, antibody-mediated tumor recognition, and autoimmune diseases such as arthritis. Recent experiments with transgenic mice have demonstrated that the FcRs control key steps in the immune response, including antibody-directed cellular cytotoxicity (ADCC) and inflammatory cascades associated with the formation of immune complexes (Ravetch and Clynes, 1998). Fc receptors that bind IgG (FcγRI, FcγRII, and FcγRIII) mediate a variety of inflammatory reactions, regulate B cell activation, and also trigger hypersensitivity through mast cells (Oettgen et al., 1994; Dombrowicz et al., 1997). FcεRI can also trigger antiparasitic reactions from platelets and eosinophils (Gounni et al., 1994; Joseph et al., 1997), as well as deliver antigen into the MHC class II presentation pathway in dendritic cells for the activation of T cells (Maurer et al., 1998).

The α subunit of the receptor binds IgE molecules with high affinity (K_d of $\sim 10^{-9}$ to 10^{-10} M) and can be secreted as a soluble, IgE-binding fragment by the introduction of a stop codon before the single C-terminal transmembrane anchor (Blank et al., 1991). The extracellular domains of the α subunit belong to the immunoglobulin (Ig) superfamily and contain seven N-linked glycosylation sites that affect the secretion and stability of the receptor (Kanellopoulos et al., 1980; LaCroix and Froese, 1993; Letourneur et al., 1995), although glycosylation of the receptor is not required for IgE binding (Robertson, 1993; Scarselli et al., 1993).

We have solved the crystal structure of the IgE-binding domains of the FcεRI α subunit. A receptor α subunit fragment expressed in insect cells yields crystals that diffract X-rays to a resolution of 2.4 Å using a high-energy synchrotron source. The receptor is formed of two truncated Ig domains that fold into a bent two-domain structure that is different from other tandem Ig domain structures. Carbohydrate moieties are observed at three of the seven N-linked attachment sites. The IgE-binding site has been identified in the second domain of the receptor and includes a prominent loop that projects from the receptor surface. The crystal structure implicates nearby residues in the first domain that may be involved in antibody binding and suggests models for the formation of a complex with the IgE-Fc region.

Results and Discussion

Structure Determination

The extracellular domains of FcεRI were expressed in different cells (Chinese hamster ovary cells, *Pichia pastoris* yeast, and *Sf9* and *Tricoplusia ni* insect cells) as

‡To whom correspondence should be addressed: (e-mail: jardetz@tochtli.biochem.nwu.edu).

Table 1. Crystallographic Data and Model Refinement

Data Collection and Analysis

	Native	Au	Pt
Resolution	2.4 Å	3.0 Å	4.0 Å
Wavelength/energy (Å/keV)	1.08/11.48	1.02/12.12	1.05/11.76
Completeness, % (last shell)	96.9 (92.5)	99.9 (100.0)	96.3 (69.9)
Ave. redundancy (last shell)	3.9 (3.4)	7.6 (7.3)	6.2 (2.7)
R_{merge}, % (last shell)	5.7 (22.6)	10.1 (39.8)	5.1 (7.0)
$<I/\sigma I>$ (last shell)	23.8 (4.5)	19.0 (3.9)	35.2 (15.9)
ΔF/F (resolution)	—	0.218 (20–3 Å)	0.093 (20–4 Å)
No. of sites	—	1	1
Phasing power acentric/centric	—	1.50/1.93	0.41/0.61
R_{cullis} acentric/centric	—	0.66/0.70	0.94/0.97
Overall figure of merit	0.487		
FOM after DM	0.673		

Refinement Statistics: 500–2.4 Å

No. of Reflections (free)	R factor/ R_{free}, %	No. of Atoms	No. of Waters	Rmsd Bonds	Rmsd Angles	Ave. B
10247 (880)	24.2/27.1	1620	126	0.0077 Å	1.53°	65.7 $Å^2$

$R_{merge} = \Sigma|I_i - <I>|/\Sigma|I|$, where I_i is the intensity of an individual reflection and $<I>$ is the average intensity of that reflection.
R factor $= \Sigma||F_p| - |F_c||/\Sigma|F_p|$, where F_c is the calculated and F_p is the observed structure factor amplitude.
Phasing power $= F_{hcalc}/E$, where F_{hcalc} = the heavy atom structure factor amplitude and E = the residual lack of closure error.
$R_{cullis} = \Sigma||F_{ph} \pm F_p| - |F_{hcalc}||/\Sigma|F_{ph} \pm F_p|$, where F_{ph} is the derivative structure factor amplitude.

variable length constructs (171, 172, and 176 amino acids of the mature protein) in order to obtain protein crystals of high quality. Glycosylation of the receptor was required to maintain protein solubility, and the variability of the glycosylation from the different cell lines affected the crystallization of the receptor (S. C. G. et al., unpublished observations). To determine the structure, several hundred crystals representing five space groups were subjected to X-ray analysis. One construct containing the first 176 amino acids of the mature receptor sequence, expressed using the baculovirus system (O'Reilly et al., 1994) in *T. ni* cells, produced significantly better crystals than other expression constructs and cell lines.

The 176/*T. ni* FcεRI crystallizes in a monoclinic crystal form (spacegroup C2) with cell dimensions 88.6 × 69.6 × 49.3 Å, $\alpha = \gamma = 90°$, $\beta = 116.7°$, and diffracts X-rays to a resolution of 2.4 Å. A native data set was collected at the Stanford Synchrotron Radiation Laboratory 7-1 beamline using a Mar300 imaging plate detector. Two derivative data sets were collected at the Dupont-Northwestern-Dow undulator beamline at the Advanced Photon Source using a MarCCD detector. The statistics for these data are shown in Table 1. In order to maximize the anomalous scattering for the two derivatives, the X-ray wavelength was set above the theoretical absorption edges of the heavy metals.

The structure of FcεRI was determined by multiple isomorphous replacement using gold and platinum heavy atom derivatives with the anomalous signal from both derivatives. The data collection and heavy atom phasing statistics are shown in Table 1. The MIRAS phases were used as input to the density modification program DM (Collaborative Computational Project, 1994), and the resultant electron density map was of sufficient quality that the entire model except for two flexible loops and five residues at the termini could be built (Figure 1A). The model was further improved by cycles of automated refinement using the program CNS (Brünger et al., 1998) followed by manual rebuilding. The current R factor and R_{free} are 24.2% and 27.1%, respectively, for all the data to 2.4 Å. No electron density is observed for three residues at the N terminus (1–3) and two residues at the C terminus (175–176), and poor density is observed for two loops (residues 32–35 and 70–73) that are disordered in the crystal. Final statistics for the model are collected in Table 1.

Overall Structure

FcεRI is composed of two Ig domains, D1 and D2, each ~85 residues in length, that are bent at an acute angle relative to each other (Figure 1C). The domain arrangement generates a convex surface at the top of the receptor that has been implicated in binding to the Fc region of the IgE antibody. The domains are small compared to canonical variable and constant Ig domains, and the shorter sequence is accommodated by truncation of the C-C′-E crossover region. Both domains D1 and D2 of FcεRI are composed of β strands AA′BCC′EFG (Figure 1D), differing from the previously described I-set domains (Harpaz and Chothia, 1994) by the absence of strand D. The nearly antiparallel domain packing places the A′B, CC′, and EF loops of D1 and the BC, C′E, and FG loops of D2 near the top of the receptor. One feature of the topology is a crossover of the A strand from the ABE sheet to the CC′FG sheet (Figures 1C and 1D), forming a short segment of parallel β sheet in an otherwise antiparallel structure. In D1 the AA′ crossover makes contacts in the D1D2 interface, while in the D2 domain residues in the A strand interact with D1 (Figure 1D).

Significant structural differences are also observed between D1 and D2. The D1 and D2 sequences contain ~28% identical residues and superimpose with an rms deviation of 1.26 Å for the Cα atoms. The F-G strands and loop differ between the two domains (Figure 1). In D2 these strands are longer, and the FG loop projects above the D2 domain surface. The C′ strands also differ between the two domains. In D2 a series of aromatic

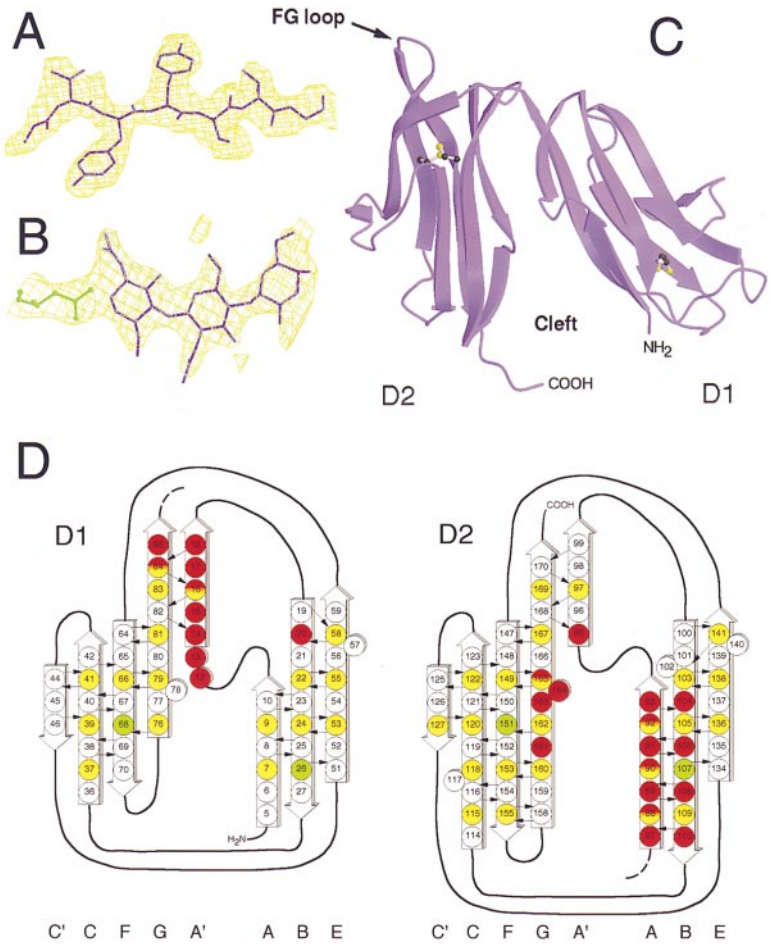

Figure 1. Electron Density Maps and Overall Structure of FcεRI

(A) The 3.0 Å experimental electron density map, calculated using the MIRAS phases followed by density modification with the program DM (Collaborative Computational Project, 1994), is shown along with the final refined model for FcεRI. The density is contoured at 1.4 σ for residues 147–153.

(B) Electron density for carbohydrate moieties linked to N42. The |2Fo-Fc| electron density map, contoured at 1 σ, was calculated to 2.4 Å using combined MIRAS and model phases (prior to inclusion of carbohydrate in the model). Two N-acetylglucosamines and a mannose moiety were built into the density as shown.

(C) Ribbon diagram of FcεRI showing the positions of the disulfides and the FG loop in domain 2 (D2) that is implicated in receptor specificity. Domain 1 (D1) is shown to the right, and D2 is shown to the left.

(D) Topology diagram of the two FcεRI domains showing the hydrogen-bonding patterns of the β sheet structure. A short stretch of parallel β sheet in D1 and D2 is caused by the cross-over of the A strand. Note that the FG strands of D2 are longer than those of D1, contributing to the prominence of the D2-FG loop. Yellow residues are buried in the protein core, red residues are at the D1D2 interface, and green residues correspond to disulfide-bonded cysteines.

residues (Y120 and Y131) form a hydrophobic core that pushes the C′ strand and loop away from the C strand, altering the local conformation of this region. The FG loop and C-C′ strands of D2 form part of the binding site for IgE.

The tertiary packing arrangement of FcεRI domains is distinct from other tandem Ig domain structures (Figures 2A and 2B). Comparison of the FcR with other bent two-Ig domain structures reveals a high degree of variability in the bend angles and packing surfaces between domains. A subset of representative structures is shown in Figure 2, including FcεRI, the natural killer cell inhibitory receptor, KIR (Fan et al., 1997), the human growth hormone receptor, HGHBP (de Vos et al., 1992), the interleukin-1 receptor, IL1R (Vigers et al., 1997), and the insect defense protein hemolin (Su et al., 1998). The proteins are oriented relative to D2 of FcεRI. The ABE half of each domain is colored yellow and the A′CC′FG half is colored blue, with light colors for domains corresponding to FcεRI D1 and dark colors for domains corresponding to FcεRI D2. FcεRI and hemolin structures have the most acute angles relating two sequential Ig domains. The top view of these domains shows that the orientations of the hemolin and FcR domains are more closely related, but between this selected subset of proteins there is significant variability in the relative orientations of tandem Ig domain structures. The bend angle between domains and domain packing interfaces are clearly unique, and this variation is likely to be important in ligand binding interactions. The FG loop of D2 in FcεRI is oriented differently with respect to D1 residues compared to the same region of the KIR or HGHBP, changing the spatial relationships of D1D2 loops that may be involved in ligand interactions.

The D1D2 Interface

The bent shape of the FcR produces a large interface between the D1D2 domains that buries 1280 Å^2 of accessible surface area of 28 D1D2 residues (Figure 3A). There are 11 residues from the D1 domain (12–18, 20, and 84–86) and 17 residues from the D2 domain that are buried at the interface (87–93, 95, 104, 106, 108, 110–111, 161, and 163–165). Of these 28 residues, 8 are completely conserved in all human FcγR and FcεR sequences (Figure 3B, residues 13, 87, 88, 90, 91, 106, 108, and 110). These conserved residues are colored yellow in Figure 3A, and they form a significant fraction of one side of the buried interface, suggesting that related FcRs would have a similar acute packing of the D1D2 domains as observed in FcεRI.

However, 20 residues that form the D1D2 interface differ in other FcRs, and these differences could alter the relative orientations of the two domains. The conserved tryptophan at position 110 packs against phenylalanine 17 in FcεRI. In other FcRs, F17 is a leucine (Figure 3B),

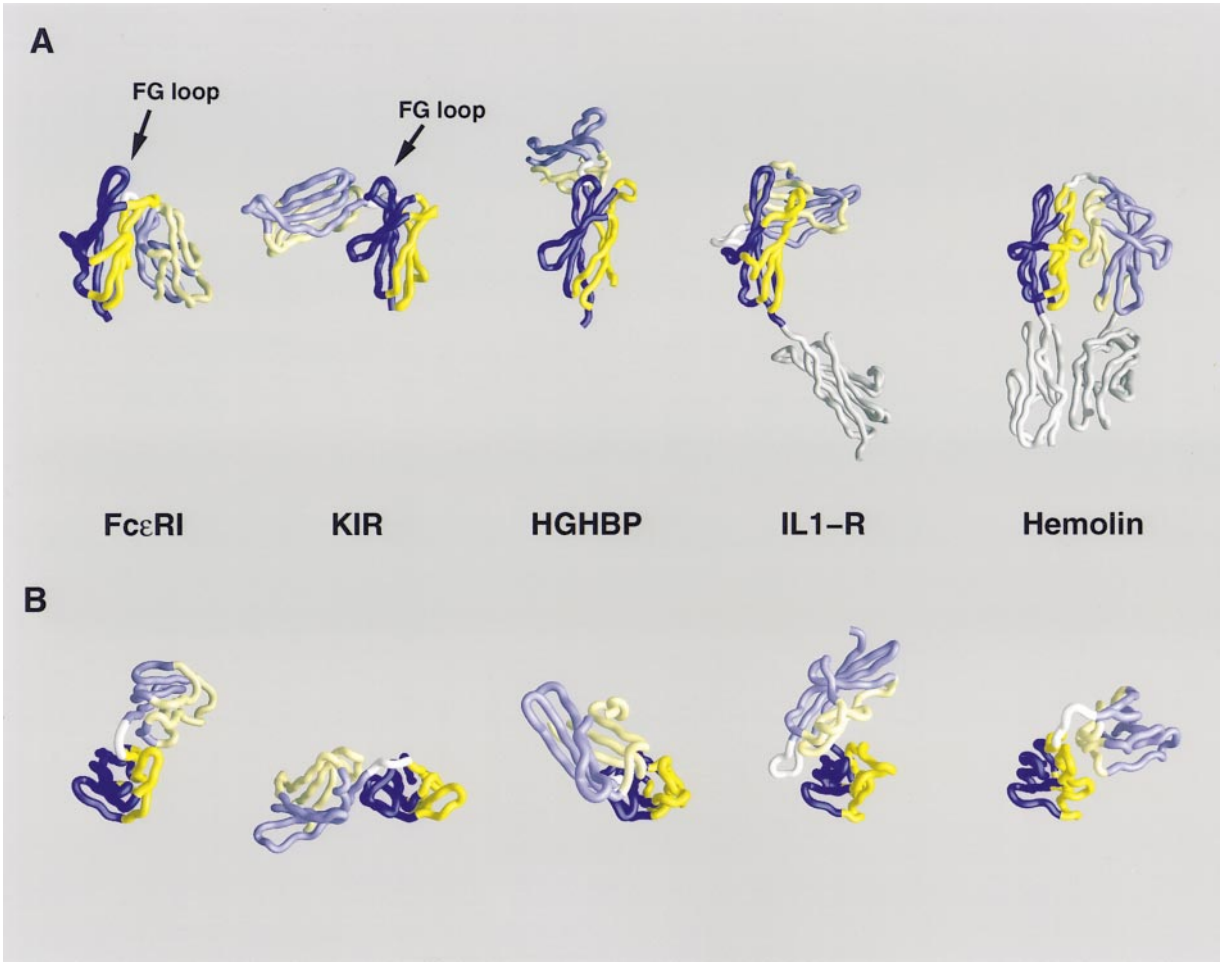

Figure 2. FcεRI Has a Novel Tertiary Arrangement of Tandem Ig Domains

(A) Side view of different tandem Ig domain arrangements in FcεRI, KIR, HGHBP, IL1-R, and hemolin. These five proteins were selected to demonstrate the variety of two sequential Ig domain arrangements with varying bend angles between domains. The five are oriented relative to FcεRI by the second C-terminal domain under comparison. The β sheets of the Ig domains are colored to clearly indicate the two faces of the domains. For the first of the two domains, the ABE sheet is colored light yellow, while the A′CC′FG sheet is colored light blue. For D2 the ABE sheet is colored dark yellow, and the A′CC′FG sheet is colored dark blue. This coloring is conserved in the four other proteins for the corresponding sheets, allowing straightforward comparison despite different sheet structures in the different Ig domains being compared. This comparison shows the variety of domain–domain angles found in tandem Ig domains.

(B) Top view of the five proteins oriented looking down the central axis of the C-terminal Ig domain. Note the variation in packing between bent Ig domains in these proteins, which includes rotational variation around the D2 axis, as well as variation in the D1 surface used to form the domain:domain interface. FcεRI packing is distinct from all of these arrangements but is most similar to the domain packing arrangement found in hemolin.

which may alter the packing of the two domains. Arg-15 forms a hydrogen bond with the carbonyl of L90 and contacts L89, F84, and L165. In other human FcRs, R15 is either serine or asparagine, changing the volume and charge at the center of the D1D2 interaction. Since the interactions of the FcR with antibody are near the D1D2 interface, alterations in residues at the interface might influence receptor specificity. Other residues that are variable among the FcR sequences in the region of the D1D2 interface could also perturb the D1D2 interactions (Figures 1D and 3B).

The bent FcR structure generates a cleft between the two domains that is near the transmembrane anchor at the C terminus of D2 (Figure 1C). This cleft is located far from the IgE-binding site identified by mutagenesis studies. Although there is no known function attributed to this region of the FcR, this surface could be a site of interaction with the extracellular regions of the β or γ subunits of the receptor. It has been suggested that interactions between the FcγRI and FcγRIIIA α and γ subunits increase the binding affinity of the receptor for IgG (Miller et al., 1996). The 5–7 extracellular amino acids of the γ chain could potentially interact with the D1D2 cleft and affect the affinity of the receptor for antibody. Recent binding studies with soluble FcεRI and IgE have also demonstrated a 10-fold lower affinity than had previously been determined in cell-binding assays (Cook et al., 1997).

Carbohydrate Attachment Sites

FcεRI is the most highly glycosylated protein structure solved by X-ray crystallography to date, having seven

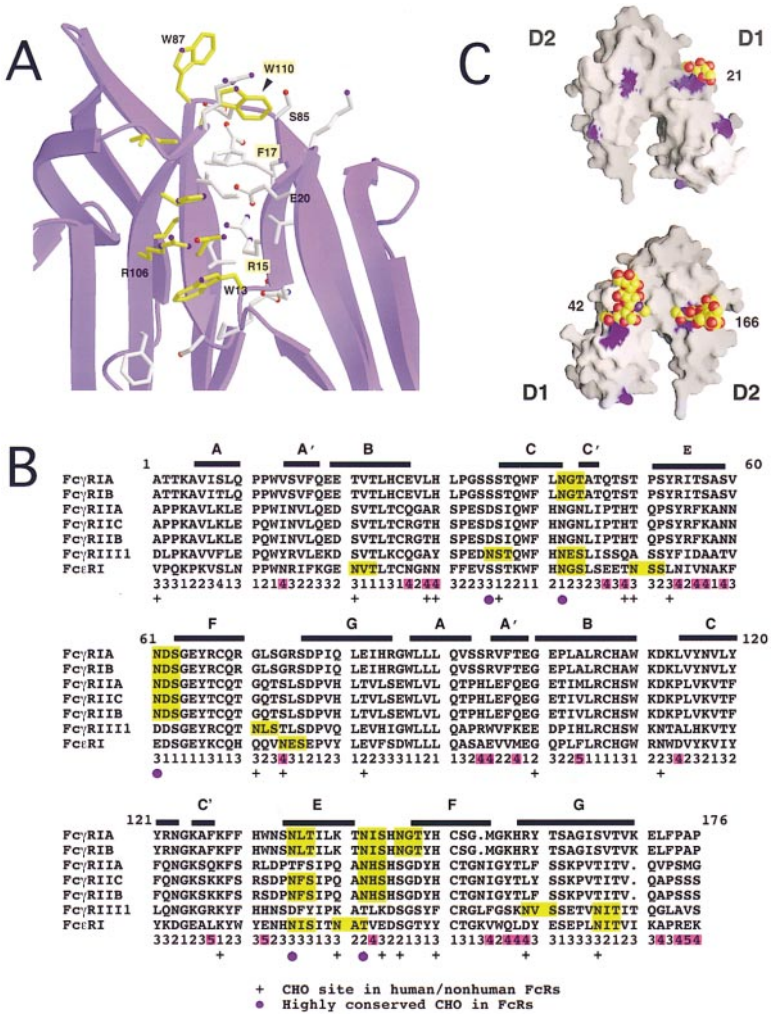

Figure 3. Sequence and Carbohydrate Attachment Site Variability in Related FcRs

(A) Amino acid interactions at the D1-D2 interface. Residues buried at the D1D2 interface are shown with absolutely conserved residues in yellow and others in white. The interaction of D1 with D2 buries 1280 Å^2 of surface area and involves 28 residues in the two domains.

(B) Sequence alignments of human Fc receptors. The sequence alignment indicates the positions of predicted carbohydrate attachment sites (highlighted in yellow for the human sequences). The secondary structure of the two domains is also indicated with labeled bars above those residues that form β sheets in FcεRI. Below the sequences, carbohydrate attachment sites found in 17 different FcR sequences are indicated with plus signs. This analysis is based on the seven human receptors shown and the nonhuman receptors in Table 2. Also shown below each residue position is the number of different amino acids found in the human IgG and IgE receptor alignment. The most variable amino acid positions (different in more than 4 of 7 sequences) are highlighted.

(C) Surface representation of FcεRI showing all of the seven carbohydrate attachment sites (blue regions of surface) and the carbohydrate structures for which interpretable electron density has been observed at residues 21, 42, and 166.

N-linked glycosylation sites in 176 amino acid residues. The intact receptor on mast cells is approximately 40% carbohydrate by weight (Kanellopoulos et al., 1980; LaCroix and Froese, 1993), with a heterogeneous molecular weight on SDS-PAGE gels of ~50 kDa. The receptor expressed in insect cells has a molecular weight of ~34 kDa as observed using SDS-PAGE, but based on typical insect cell glycosylation structures (-GlcNAc$_2$-Man$_3$-GlcNAc), it could be expected to have a molecular weight of ~27.5 kDa, or approximately 30% carbohydrate by weight. While the presence of carbohydrate at these seven sites is not required for binding to IgE (Robertson, 1993; Scarselli et al., 1993; Letourneur et al., 1995), mutation of these sites or treatment of FcR-expressing cells with tunicamycin leads to the aggregation of the receptor during biosynthesis.

In the FcεRI crystal structure, carbohydrate density is observed at three of the seven predicted glycosylation sites (Figure 3C, residues 21, 42, and 166). For two of these sites, Asp-42 and Asp-166, three sugar moieties were built. The carbohydrate at position 42 extends up toward the top of the FcεRI structure, covering residues F60, S63, and V83. The carbohydrate attached to position 166 projects away from the protein surface, potentially as a result of crystal contacts and the modification of the 3 and 6 positions of the first GlcNac residue. The other carbohydrate sites are indicated on the FcεRI surface as blue regions of the surface. No interpretable density is observed for these glycosylation sites.

Many of the related FcRs are also highly glycosylated proteins, and the glycosylation sites vary between receptors. The rat and mouse FcεRIs each have six potential N-linked glycosylation sites, but the rat receptor has only two sites and the mouse receptor only one site in common with the human receptor. Comparison of 17 human and animal FcR sequences identifies 25 different potential N-linked carbohydrate attachment sites in related FcRs (Figure 3B). The 25 sites are distributed evenly between D1 and D2, with 14 sites in D1 and 11 sites in D2. Five of these sites are relatively well conserved sites in all FcRs (found in >9/17 sequences analyzed), corresponding to residues 35, 42, 61, 135, and 142 (Figure 3B). The distribution of all of the sites on the surface of FcεRI is shown in Figure 4A (gray Cα positions). These sites cover a significant fraction of the FcεRI surface on both major faces of D1 and D2, placing limitations on the FcR surface available for interactions with antibody.

The Receptor-Binding Site for IgE

A number of mutagenesis studies have been carried out to elucidate the regions of FcεRI that are critical for the

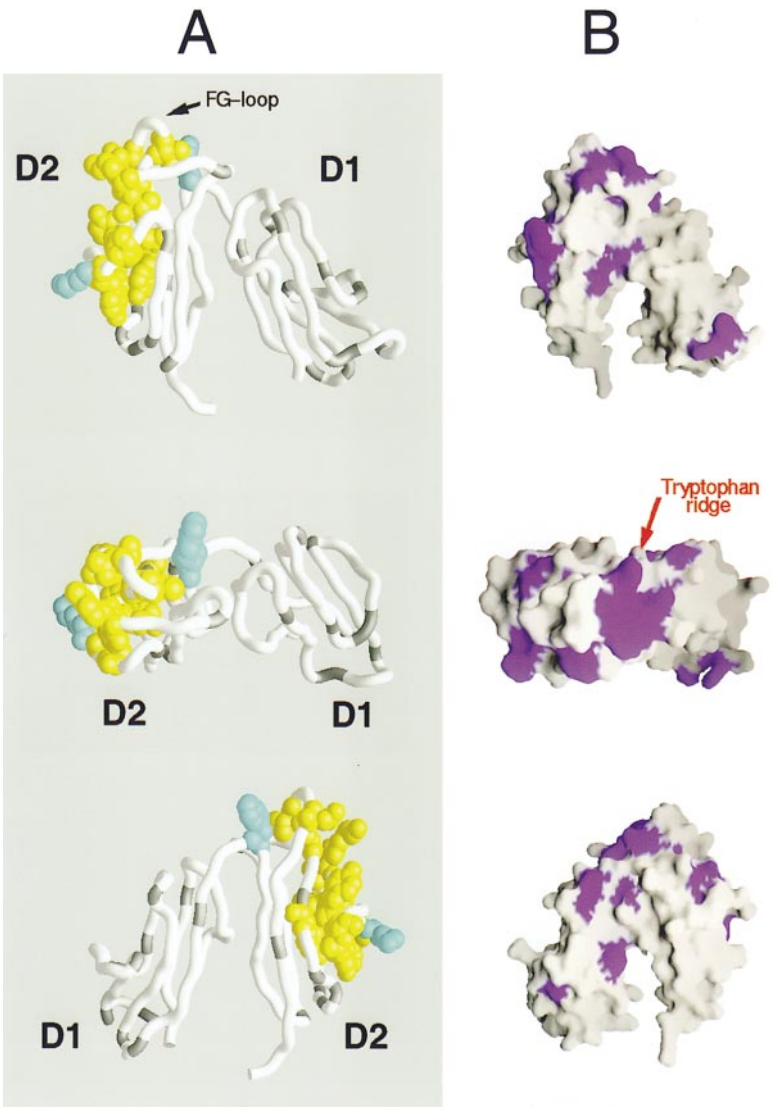

Figure 4. Identification of the FcεRI-Binding Site for IgE

(A) Residues of FcεRI implicated in binding IgE, shown in three orientations of the receptor (side and top views). Residues that have been identified by mutagenesis studies in forming the binding site for the IgE-Fc are shown in yellow. Two residues that affect FcεRI binding to a mutant IgE-Fc (R334S) are shown in magenta. Carbohydrate attachment sites for all of the human and nonhuman receptors in Table 2 are colored gray in the Cα track. Note that the carbohydrate sites cover a substantial portion of the FcR surface, but they do not impinge on the binding site region identified by mutagenesis.

(B) A surface representation of the IgE receptor showing the surface exposure of aromatic residues in blue. The patch corresponding to the four tryptophans is indicated. Aromatic residues that form part of the predicted IgE-binding site are also evident in the D2 C-C′ region.

interaction with IgE molecules (Hulett et al., 1993, 1994, 1995; Mallamaci et al., 1993; Cook et al., 1997). These experiments have demonstrated an important role for amino acids in the D2 domain of the receptor, although some regions of D1 are also likely to be involved in IgE binding. Current evidence that D1 plays a role in IgE binding includes the deletion of D1 (Robertson, 1993; Scarselli et al., 1993) or substitution with a homologous IgG receptor (Hulett et al., 1994). These experiments do not determine conclusively whether D1 interacts directly with the IgE or whether D1 indirectly alters the structure of D2 and subsequent interactions with IgE. The substitution or elimination of residues at the D1D2 interface (Figure 3B) could potentially influence D2 interactions with antibody Fc regions. There are a number of regions of D1 that have been excluded from determinants of the specificity of the receptor for IgE, since these FcεRI segments can be substituted by the corresponding residues in the FcγRIIIA protein (Mallamaci et al., 1993), including residues 25–38, 43–54, 67–79, and 77–86. Substitution of residues 10–21 or 55–67 disrupts the binding of IgE and five different monoclonal antibodies, suggesting that residue differences in these segments may affect the folding of hybrid molecules.

FcεRI residues that have been implicated in IgE binding include residues in the D2 C strand (115, 117, 118, and 120–123), the C′-E loop (129 and 131), the F strand (149 and 153), the FG loop (155), and the G strand (159) (Hulett et al., 1994, 1995; Cook et al., 1997). In addition, residues 87 (at the D1D2 interface) and 128 (in the C′-E loop) are likely to be part of the IgE interaction site, since mutation of these residues influences receptor binding to the IgE point mutant R334A (Cook et al., 1997). Of these 15 residues, 6 are buried in the protein core, and substitution may lead to indirect structural changes that affect IgE binding (115, 118, 120, 131, 149, and 155). Three of the residues are either partially buried or glycine and substitution may affect the conformation of the local residues (122, 129, and 153). The remaining residues (87, 117, 121, 123, 128, and 159) are all exposed amino acids at the FcεRI surface. A synthetic peptide containing residues 119–129 has been demonstrated to

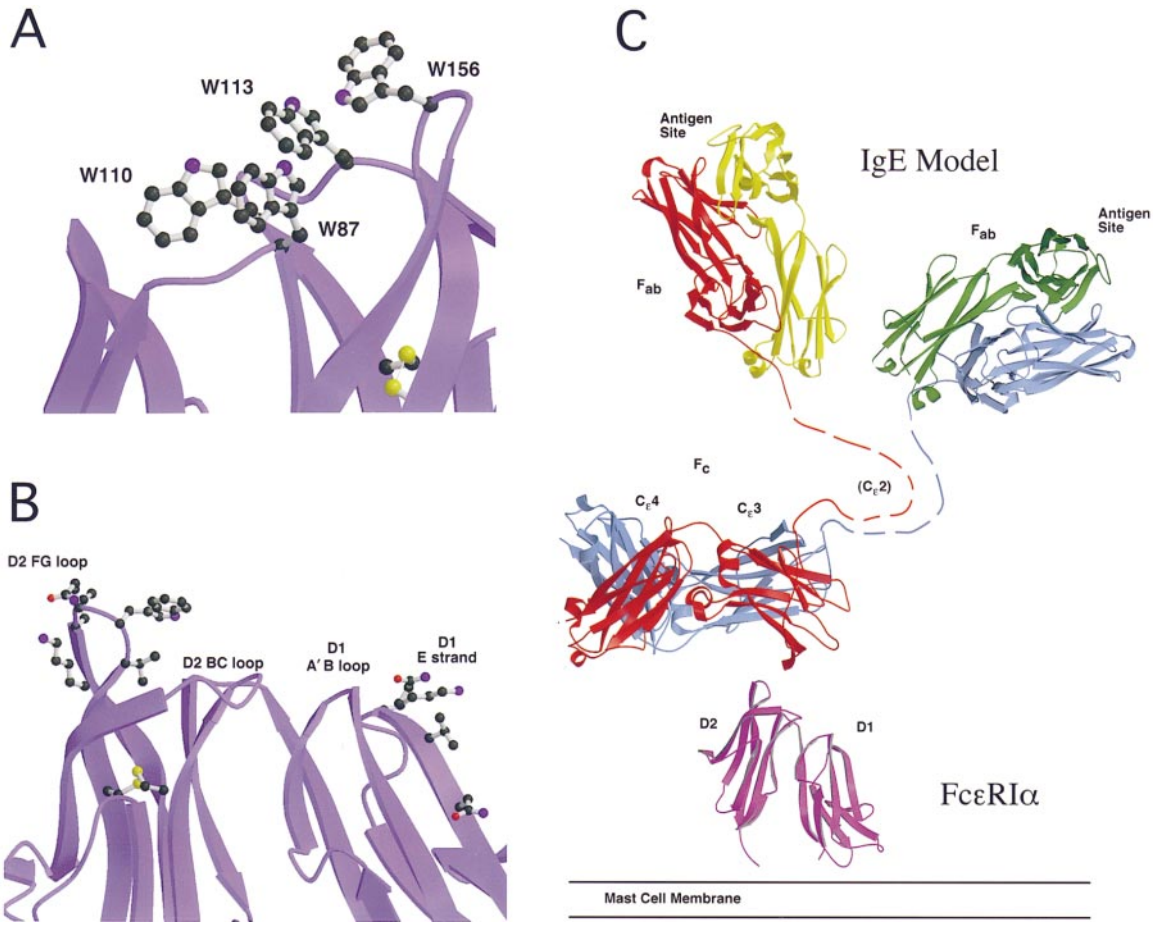

Figure 5. Implications for FcεRI Specificity and Its Interaction with IgE

(A) Four surface-exposed tryptophans at the top of the D2 domain that are implicated in IgE binding.

(B) Residues in the D2-FG loop and D1-E strand that are highly variable in human FcR sequences. The residues in the D2-FG loop have been directly implicated in IgE binding (see text). The residues in the D1-E strand and the D1-A′B loop are located near the top of the D2 domain and could form part of an extended IgE-binding surface between the two domains. Note that the carbohydrate attachment sites shown in Figure 4A are consistent with a continuous Fc-binding surface spanning the two domains involving these D1 loop regions.

(C) Juxtaposition of FcεRI with a model for the intact IgE antibody structure. The IgE model is derived from the intact IgG1 antibody (Harris et al., 1998). The insertion of the Cε2 domains in the IgE molecule is indicated by dotted lines. The FcεRI α chain is shown relative to the mast cell membrane near the top of the Cε3 domains that bind to the receptor.

block IgE binding to the receptor, with a K_d of ~3 μM (McDonnell et al., 1996, 1997). The implicated residues (Figure 4A) form a contiguous surface extending from the back side of the D2 domain to the top region near the D1D2 interface. Four of the residues are conserved in all human FcRs (87, 118, 149, and 153) and may define a set of common interactions between all FcR receptors and their target Ig molecules.

The region of the D2 domain defined by mutagenesis also borders on a number of surface-accessible aromatic residues, including four prominent tryptophans at the top of the FcR molecule, residues 87, 110, 113, and 156. Figure 4B shows a surface representation of all of the exposed aromatic groups of the FcR, outlining the tryptophan ridge and residues in D2 near the CC′-E region that has been identified by mutagenesis studies. The four tryptophans are shown in Figure 5A, forming a flat, hydrophobic ridge that neighbors the D2 FG loop. This unusual arrangement of four exposed tryptophans probably forms a contact surface for a complementary interaction with the IgE. Trp-87 has already been implicated by mutagenesis studies, and Trp-156 is prominently displayed at the top of the FG loop. Trp-156 is a glycine in all IgG-FcRs (Figure 3B), and grafting of FcεRI FG-loop (residues 154–161) to the FcγRII IgG-FcR confers IgE binding.

Implications for the Binding Specificity of Fc Receptors

Since carbohydrate would be expected to disrupt any closely packed protein:protein interface, it is interesting to compare the known carbohydrate sites with the proposed IgE-binding site on the receptor surface. All of the carbohydrate attachment sites for 17 related FcRs are shown in Figure 4A, demonstrating that the N-linked carbohydrate sites delineate a boundary around the proposed IgE-binding site. This is consistent with related FcRs sharing a common binding surface for antibody

molecules. Studies of the FcγRII specificity for IgG have implicated residues in the same region of the receptor, including residues 113–116, 129, 131, 133, 134, 155, 156, and 159–161 (Hulett et al., 1994, 1995). In addition, many domain-swap experiments have demonstrated that two of the related IgG-FcRs can form functional hybrid molecules with FcεRI (Mallamaci et al., 1993; Hulett et al., 1995), suggesting that these receptors share a common binding surface with their respective antibody ligands.

The top of the FcR structure is devoid of carbohydrate attachment sites in the region of D2 that has been implicated in direct interactions with Ig molecules. The neighboring surface of the D1 domain, including loops A′B and EF, is also devoid of carbohydrate and could form part of an extended antibody-binding site across the D1D2 interface. If these D1 loops are important in determining the specificity and affinity of the FcR:antibody interaction, one might observe sequence variability between high- and low-affinity IgG receptors and the IgE receptor. This variability in the human IgG and IgE receptors is shown in Figure 3B. For residues 3–173, there are 73 amino acid differences that are unique to FcεRI compared to the IgG receptors, and there are five regions that stand out with clusters of sequence variability: residues 27–30, 47–49, 54–59, 94–98, and 155–159. Residues 155–159 (the FG loop) are highly variable and at least partially determine the specificity of FcR interactions.

Previous experiments have shown that residues 27–30 and 47–49 are not critical for FcR specificity (Mallamaci et al., 1993), and the presence of glycosylation sites within these segments in related FcRs (Figure 3B) supports the suggestion that these regions are not part of the FcR:antibody interaction. Residues 94–98 are found in the A′ strand near the D1D2 cleft and therefore are not likely to interact with antibody directly, but these residues might influence interactions indirectly by altering the D1D2 packing interface.

The remaining group of highly variable residues (54–59) are in the D1 E strand (Figure 5B), near the FcεRI-binding site. Residues 54–59 could form a D1 surface of interaction with the Ig-Fc domains, extending the binding site across both FcR domains. Since exchange of FcεRI residues 55–67 with residues from the FcγRIIIA receptor may disrupt the folding of the protein (Mallamaci et al., 1993), targeted point mutations may be required to test the importance of residues in the D1-E strand. The neighboring D1 A′B loop (residues 18–21) could also form part of an extended surface of interaction with the antibody.

Conclusions

The activation of Fc receptor bearing cells requires cross-linking of the receptors, which leads to the activation of intracellular kinase cascades analogous to those in B and T cells (Metzger, 1992; Daeron, 1997). For both high- and low-affinity receptors (the FcεRI and FcγRIII), a stoichiometry of 1:1 is observed between the receptor and the Ig-Fc region (Kanellopoulos et al., 1980; Ghirlando et al., 1995; Keown et al., 1997), consistent with a requirement for antigen to cause receptor aggregation and activation. The binding site on the IgE-Fc for its receptor has been extensively studied by mutagenesis, implicating amino acids in the third constant domain (Cε3) of the IgE (Nissim et al., 1991; Basu et al., 1993; Presta et al., 1994; Henry et al., 1997). The structure of the IgE-Fc region has not been experimentally determined but is homologous to the IgG-Fc, for which a number of crystal structures are available. The IgG-Fc-binding site for the FcγRI and FcγRII receptors has been mapped to a similar, although smaller, surface that primarily includes residues in the hinge region before the Cγ2 domain (Duncan et al., 1988; Jefferis et al., 1990; Canfield and Morrison, 1991; Lund et al., 1991).

The antibody Fc region is a homodimeric structure that is significantly larger than the Fc receptor (Figure 5C). The observed 1:1 stoichiometry between receptor and antibody indicates that the two-fold symmetry of the Fc region does not lead to the binding of two FcRs, even with isolated molecules in solution. The large and convex nature of the FcR-binding surface could span two antibody domains (Cγ2 in IgG and Cε3 in IgE) and induce a conformational change in the Fc that would prevent the binding of a second FcR to the same antibody. The FcR structure could also form an asymmetric complex with the antibody that sterically blocks the binding of a second FcR, perhaps using the protruding FG loop to block symmetric interactions with the Fc hinge region.

The FcRs vary in their level of glycosylation. In FcεRIα the number of glycosylation sites (6–7) is maintained, but the position of these sites varies. In the human FcRs, the number of glycosylation sites shows some correlation with binding affinity (Table 2). The high-affinity FcRs, which can bind Ig prior to the binding of antigen, typically have 5–7 potential glycosylation sites. Low-affinity FcRs, which bind Ig–antigen aggregates, have as few as two sites. Since FcR activation requires cross-linking of receptors, glycosylation might prevent the aggregation of large antibodies at the cell surface bound by high-affinity FcRs. Lipid/water interfaces can enhance the crystallization of proteins (Hemming et al., 1995), and the potentially high local concentrations of membrane-bound Ig might lead to FcR activation in the absence of antigen. The low-affinity IgG receptors interact with antibody–antigen aggregates that can simultaneously bind and activate multiple FcRs. In these receptors, glycosylation may not be quite as important, since interaction with the antibody could occur after the binding of antigen.

There may be other roles for the FcR glycosylation, since the nonhuman FcRs (Table 2) do not show an obvious correlation of the number of carbohydrate sites and FcR affinity. Glycosylation might be important in FcR signaling by orienting receptor:antibody complexes into functional signaling complexes (i.e., by preventing antigen-cross-linked complexes from forming nonfunctional aggregates). It is known that activation through the IgE receptor is sensitive to geometrical constraints imposed by antigen cross-linkers, although the nature of these physical constraints is poorly understood. The recent crystal structure determination of an erythropoeitin–receptor complex suggests that the orientation of ligand-mediated dimerization of cell-surface receptors may be important in efficient signal transduction (Syed et al., 1998).

Table 2. FcR Glycosylation Sites and Ig Binding Affinity

FcR	No. of CHO Sites (Total)	Affinity
Human		
FcεRI	7	High (10^{-9}–10^{-10}M)
FcγRIA (CD64)	5 (7)	High (3 domains, 10^{-8}–10^{-9}M)
FcγRIB (CD64)	5 (7)	High (3 domains, 10^{-8}–10^{-9}M)
FcγRIIA (CD32)	2 (3)	Low (10^{-6}M)
FcγRIIB (CD32)	3	Low (10^{-6}M)
FcγRIIC (CD32)	3 (4)	Low (10^{-6}M)
FcγRIIIA (CD16)	5 (6 in variant)	Low (10^{-6}M)
Mouse		
FcεRI	6	High (10^{-9}–10^{-10}M)
FcγRI	4 (5)	High (3 domains, 10^{-7}–10^{-8}M)
FcγRIIb	4 (5)	Low (10^{-6}M)
FcγRIIIa	4	Low (10^{-6}M)
Rat		
FcεRI	7	High (10^{-9}–10^{-10}M)
FcγRII	6 (7 total)	Low
FcγRIII	5	Low
Other		
FcγRII (guinea pig)	5 (6)	Low
FcγRIII (pig)	3	Low
FcγRII (bovine)	6	Low

Comparison of the number of predicted glycosylation sites and the affinity of different FcRs for antibody. The number of glycosylation sites in the domains corresponding to the extracellular fragment of the human FcεRI are shown along with the total number of glycosylation sites in parentheses. The affinities quoted are taken from Ravetch and Clynes (1998) and Ravetch and Kinet (1991).

Although the receptor-binding site for IgE is overall broad and convex in shape, there are regions on the surface of the receptor that are candidate targets for small molecule inhibitors. Crystal packing interactions with the four exposed tryptophans show that small hydrophobic groups can interact with the adjacent indole moeities at the top of the IgE-binding site. Other grooves or pockets on the FcR surface might also bind potential small molecule inhibitors, such as the C-strand region of D2 or the D1D2 cleft.

Experimental Procedures

Expression and Purification of the Human High-Affinity IgE Receptor

The human FcεRIα protein was expressed in insect cells using the baculovirus expression system. The construction and expression of this and other vectors for the FcεRIα will be described in detail elsewhere (S. C. G. et al., unpublished data). Briefly, DNA including the wild-type receptor signal sequence and first 176 amino acids of the mature receptor α chain were cloned into the pVL1392 baculovirus transfer vector (Pharmingen). An EcoRI-HindIII fragment from plasmid EdpC20 (Blank et al., 1991) containing the receptor signal sequence and residues 1–172 was ligated to two oligonucleotides coding for the receptor residues 172–176 and two stop codons. The synthetic oligonucleotides (5′-agctCCGCGT GAGAAGTAAT AAG-3′ and 5′-gatcCTTATT ACTTCTCACG CGG-3′) have HindIII and BamHI overhangs when annealed together, allowing the subcloning of the 1–176 construct in EcoRI-BamHI cleaved pVL1392. The resultant construct was verified by DNA sequencing. Recombinant baculovirus expressing the receptor was generated using the Baculogold transfection system (Pharmingen). Supernatants of transfected Sf9 cells were amplified once in TNM-FH medium (Pharmingen), followed by a second amplification in serum-free medium (SF-900, GIBCO). For each virus stock used in protein production, the optimal amount of virus and harvest time postinfection was determined by small scale tests in 50 ml shaker flasks.

T. ni (Hi-5) cells grown in shaker or spinner flasks were used for protein production and purification. Typical yields for protein expression were 2–12 mg/l of infected cells 2–4 days after infection. Supernatants from 1.5–5 l of Hi-5 cells were collected, filtered through 0.2 micron filters, and loaded onto a Mab15-1 (Sechi et al., 1996) monoclonal antibody column. Supernatants were recirculated over the column at least twice, followed by buffer washes (~300 ml, 100 mM Na, KPO_4 [pH 7]), until the absorbance at 280 nm of the eluant returned to zero. The protein was eluted by two urea washes: 100 ml of 5 M urea in 100 mM phosphate (pH 7.0), then 100 ml of 7 M urea in 100 mM phosphate (pH 7.0), followed by extensive regeneration with 100 mM Na, KPO_4 (pH 7.0). The urea eluants were pooled, concentrated to ~25–40 ml with an Amicon stirring concentrator, and dialyzed four times against 2 l of 50 mM Tris (pH 7.5). The purity was verified by SDS-PAGE and protein stored at 4°C for crystallization in the presence of 0.05% sodium azide. Final yield of the protein was ~50% based on an absorption coefficient of 2.6 $(mg^{-1})(cm^2)$ for the purified protein and the total protein estimated using ELISA assays with the initial cell supernatants.

FcR ELISA Assay

An inhibition-ELISA assay was used to quantitate receptor expression. The binding of Mab15-1 antibody to plate-bound FcεRI is monitored using a goat anti-mouse-alkaline phosphatase antibody (Sigma, A-2429). Unknown samples compete for antibody binding and are compared to a standard curve. Fifty microliters of purified FcεRI was incubated in microtiter plates o/n at 4°C at a concentration of 1 μg/ml in phosphate-buffered saline. Plates were rinsed with wash buffer containing 20 mM HEPES 7.5, 100 mM NaCl, 0.1% Tween-20, and blocked with HEPES/NaCl buffer with 1% Carnation dry milk. Standard inhibitor samples ranging from 0.1–50 μg/ml of FcεRI in two-fold dilution series were incubated with Mab15-1 (0.1 μg/ml final concentration) and added in duplicate to wells coated with FcεRI. Standard controls included wells without o/n incubation with FcεRI, and addition of Mab15-1 without inhibiting FcεRI. Secondary antibody in a 1:5000 dilution was incubated after washing for 1–2 hr at room temperature. Plates were washed and developed using the AP reagent p-nitrophenyl phosphate (PNPP, Sigma 104–105). Microplates were read using a Molecular Devices SpectraMax Plus reader at 405 nm.

Crystallization and Data Collection

Purified FcεRIα was concentrated to a final concentration of 20 mg/ml in 20 mM Tris (pH 7.5). Crystallization was carried out using the hanging drop method, with a precipitant composed of 100 mM Tris (pH 8.5), 200 mM NaOAc, and 18%–24% PEG 4000. Crystals were obtained in 2–10 days amid significant amounts of protein precipitate. At lower PEG concentrations a different crystal form is observed. The crystals used in the structure determination typically grow as clusters of 3–20 crystals that can be separated manually. The crystals belong to the monoclinic space group C2, with cell dimensions 88.6 × 69.6 × 49.3 Å, $\alpha = \gamma = 90°$, $\beta = 116.7°$, with one receptor molecule per asymmetric unit.

Crystals were harvested into harvest buffer containing 35% PEG 4000, 100 mM Tris (pH 8.5). For data collection, crystals were mounted in nylon loops (Hampton-Research) and rapidly cooled in liquid nitrogen after a short (~30 s) soak in harvest buffer supplemented with 14% glycerol. Heavy atom soaks with K_2PtBr_4 and K_3AuCl_3 were done in harvest buffer with 5 mM Pt for 48 hr and 1 mM Au for 18 days. Data were collected at the Stanford Synchrotron Radiation Laboratories (SSRL) 7-1 beamline and at the Dupont-Northwestern-Dow undulator beamline at the Advanced Photon Source at Argonne National Laboratories (Table 1). For the Pt and Au data sets, the wavelength was chosen to be 200 eV above the absorption edge of the metal, in order to maximize the anomalous signal for each heavy atom. Heavy atom data were collected using reverse beam protocols to optimize the anomalous diffraction signal.

Diffraction data were collected with a Mar300 Image plate (SSRL) or a MarCCD detector (DND-CAT), and integrated and scaled with DENZO/SCALEPACK (Otwinowski and Minor, 1997). The CCP4 suite of programs (Collaborative Computational Project, 1994) was used for further processing and identification of heavy atom sites.

MIR Phasing and Structure Refinement

Heavy atom positions were identified from peaks in the anomalous and isomorphous difference patterson maps. Heavy atom positions were refined and phases calculated with the program MLPHARE, followed by solvent flattening and density modification with the program DM. The subsequent model was refined using the CNS program (Brünger et al., 1998) with the combined maximum likelihood and experimental phase target (MLHL). The model was refined against all data from 500 to 2.4 Å using a bulk solvent model. Refinement steps were accepted only when they produced a decrease in the R_{free}. Since refinement of restrained temperature factors for every atom did not lead to a decrease in R_{free}, only two thermal parameters per amino acid were allowed. The model contains one residue (Trp-156) in the disallowed region of the Ramachandran diagram. Current refinement statistics are listed in Table 1.

Figures were generated with the programs O (Jones et al., 1991), MOLSCRIPT (Kraulis, 1991), Raster3d (Merritt and Bacon, 1997), and GRASP (Nicholls et al., 1991).

Acknowledgments

We would thank Beth Wurzburg and Kent Baker for help in synchrotron data collection and useful discussions, Eunjoo Song and Svetlana Tarchevskaya for their help in protein preparation, Marie-Helene Jouvin for providing the EdpC20 vector, Salvatore Sechi for prior efforts in the crystallization of the receptor, and Joshua Schnell and Susan McGovern for contributions to the project. We are particularly grateful to John Quintana and Denis Keane of the Dupont-Northwestern-Dow (DND-CAT) beamline for assistance in data collection. Portions of this work were performed at the DND-CAT Synchrotron Research Center of the Advanced Photon Source and at the Stanford Synchrotron Radiation Laboratory (SSRL), which is operated by the Department of Energy, Office of Basic Energy Sciences. This research has been supported by National Institutes of Health grant AI-38972 (T. S. J.), the Pew Scholars Program in the Biomedical Sciences (T. S. J.), the Heska Corporation (T. S. J.), and a postdoctoral fellowship award from the American Cancer Society (S. C. G.).

Received November 5, 1998; revised November 24, 1998.

References

Basu, M., Hakimi, J., Dharm, E., Kondas, J.A., Tsien, W.H., Pilson, R.S., Lin, P., Gilfillan, A., Haring, P., Braswell, E.H., et al. (1993). Purification and characterization of human recombinant IgE-Fc fragments that bind to the human high affinity IgE receptor. J. Biol. Chem. *268*, 13118–13127.

Blank, U., Ra, C.S., and Kinet, J.P. (1991). Characterization of truncated alpha chain products from human, rat, and mouse high affinity receptor for immunoglobulin E. J. Biol. Chem. *266*, 2639–2646.

Brünger, A.T., Adams, P.D., Clore, G.M., DeLano, W.L., Gros, P., Grosse-Kunstleve, R.W., Jiang, J.S., Kuszewski, J., Nilges, M., Pannu, N.S., et al. (1998). Crystallography and NMR system: a new software suite for macromolecular structure determination. Acta Crystallogr. D Biol. Crystallogr. *54*, 905–921.

Canfield, S.M., and Morrison, S.L. (1991). The binding affinity of human IgG for its high affinity Fc receptor is determined by multiple amino acids in the CH2 domain and is modulated by the hinge region. J. Exp. Med. *173*, 1483–1491.

Collaborative Computational Project, Number 4. (1994). The CCP4 suite: programs for protein crystallography. Acta Crystallogr. *D50*, 760–763.

Cook, J.P., Henry, A.J., McDonnell, J.M., Owens, R.J., Sutton, B.J., and Gould, H.J. (1997). Identification of contact residues in the IgE binding site of human FcεRIα. Biochemistry *36*, 15579–15588.

Cookson, W.O., and Moffatt, M.F. (1997). Asthma: an epidemic in the absence of infection? Science *275*, 41–42.

Daeron, M. (1997). Fc receptor biology. Annu. Rev. Immunol. *15*, 203–234.

de Vos, A.M., Ultsch, M., and Kossiakoff, A.A. (1992). Human growth hormone and extracellular domain of its receptor: crystal structure of the complex. Science *255*, 306–312.

Dombrowicz, D., Flamand, V., Brigman, K.K., Koller, B.H., and Kinet, J.P. (1993). Abolition of anaphylaxis by targeted disruption of the high affinity immunoglobulin E receptor alpha chain gene. Cell *75*, 969–976.

Dombrowicz, D., Flamand, V., Miyajima, I., Ravetch, J.V., Galli, S.J., and Kinet, J.P. (1997). Absence of FcεRIα chain results in upregulation of FcγRIII-dependent mast cell degranulation and anaphylaxis. Evidence of competition between FcεRI and FcγRIII for limiting amounts of FcR beta and gamma chains. J. Clin. Invest. *99*, 915–925.

Duncan, A.R., Woof, J.M., Partridge, L.J., Burton, D.R., and Winter, G. (1988). Localization of the binding site for the human high-affinity Fc receptor on IgG. Nature *332*, 563–564.

Fan, Q.R., Mosyak, L., Winter, C.C., Wagtmann, N., Long, E.O., and Wiley, D.C. (1997). Structure of the inhibitory receptor for human natural killer cells resembles haematopoietic receptors. Nature *389*, 96–100.

Ghirlando, R., Keown, M.B., Mackay, G.A., Lewis, M.S., Unkeless, J.C., and Gould, H.J. (1995). Stoichiometry and thermodynamics of the interaction between the Fc fragment of human IgG1 and its low-affinity receptor FcγRIII. Biochemistry *34*, 13320–13327.

Gounni, A.S., Lamkhioued, B., Ochiai, K., Tanaka, Y., Delaporte, E., Capron, A., Kinet, J.P., and Capron, M. (1994). High-affinity IgE receptor on eosinophils is involved in defence against parasites. Nature *367*, 183–186.

Harpaz, Y., and Chothia, C. (1994). Many of the immunoglobulin superfamily domains in cell adhesion molecules and surface receptors belong to a new structural set which is close to that containing variable domains. J. Mol. Biol. *238*, 528–539.

Harris, L.J., Skaletsky, E., and McPherson, A. (1998). Crystallographic structure of an intact IgG1 monoclonal antibody. J. Mol. Biol. *275*, 861–872.

Hemming, S.A., Bochkarev, A., Darst, S.A., Kornberg, R.D., Ala, P., Yang, D.S., and Edwards, A.M. (1995). The mechanism of protein crystal growth from lipid layers. J. Mol. Biol. *246*, 308–316.

Henry, A.J., Cook, J.P., McDonnell, J.M., Mackay, G.A., Shi, J., Sutton, B.J., and Gould, H.J. (1997). Participation of the N-terminal region of Cε3 in the binding of human IgE to its high-affinity receptor FcεRI. Biochemistry *36*, 15568–15578.

Hill, M.R., and Cookson, W.O. (1996). A new variant of the beta subunit of the high-affinity receptor for immunoglobulin E (FcεRI-β E237G): associations with measures of atopy and bronchial hyperresponsiveness. Hum. Mol. Genet. *5*, 959–962.

Hill, M.R., James, A.L., Faux, J.A., Ryan, G., Hopkin, J.M., le Souef, P., Musk, A.W., and Cookson, W.O. (1995). FcεRI-β polymorphism and risk of atopy in a general population sample. BMJ *311*, 776–779.

Hulett, M.D., McKenzie, I.F., and Hogarth, P.M. (1993). Chimeric Fc receptors identify immunoglobulin-binding regions in human FcγRII and FcεRI. Eur. J. Immunol. *23*, 640–645.

Hulett, M.D., Witort, E., Brinkworth, R.I., McKenzie, I.F., and Hogarth, P.M. (1994). Identification of the IgG binding site of the human low affinity receptor for IgG FcγRII. Enhancement and ablation of binding by site-directed mutagenesis. J. Biol. Chem. *269*, 15287–15293.

Hulett, M.D., Witort, E., Brinkworth, R.I., McKenzie, I.F., and Hogarth, P.M. (1995). Multiple regions of human FcγRII (CD32) contribute to the binding of IgG. J. Biol. Chem. *270*, 21188–21194.

Jefferis, R., Lund, J., and Pound, J. (1990). Molecular definition of interaction sites on human IgG for Fc receptors (huFc gamma R). Mol. Immunol. *27*, 1237–1240.

Jones, T.A., Zou, J.Y., Cowan, S.W., and Kjeldgaard, M. (1991). Improved methods for building protein models in electron density maps and the location of errors in these models. Acta Crystallogr. A *47*, 110–119.

Joseph, M., Gounni, A.S., Kusnierz, J.P., Vorng, H., Sarfati, M., Kinet,

J.P., Tonnel, A.B., Capron, A., and Capron, M. (1997). Expression and functions of the high-affinity IgE receptor on human platelets and megakaryocyte precursors. Eur. J. Immunol. *27*, 2212–2218.

Kanellopoulos, J.M., Liu, T.Y., Poy, G., and Metzger, H. (1980). Composition and subunit structure of the cell receptor for immunoglobulin E. J. Biol. Chem. *255*, 9060–9066.

Keown, M.B., Ghirlando, R., Mackay, G.A., Sutton, B.J., and Gould, H.J. (1997). Basis of the 1:1 stoichiometry of the high affinity receptor FcεRI-IgE complex. Eur. Biophys. J. *25*, 471–476.

Kim, H.S., Tsai, P.B., and Oh, C.K. (1998). The genetics of asthma. Curr. Opin. Pulm. Med. *4*, 46–48.

Kraulis, P.J. (1991). MOLSCRIPT: a program to produce both detailed and schematic plots of protein structures. J. Appl. Crystallogr. *24*, 946–950.

LaCroix, E.L., and Froese, A. (1993). The N-linked oligosaccharides of the Fc epsilon receptors of rat basophilic leukemia cells. Mol. Immunol. *30*, 321–330.

Letourneur, O., Sechi, S., Willette-Brown, J., Robertson, M.W., and Kinet, J.P. (1995). Glycosylation of human truncated FcεRI alpha chain is necessary for efficient folding in the endoplasmic reticulum. J. Biol. Chem. *270*, 8249–8256.

Lund, J., Winter, G., Jones, P.T., Pound, J.D., Tanaka, T., Walker, M.R., Artymiuk, P.J., Arata, Y., Burton, D.R., Jefferis, R., et al. (1991). Human FcγRI and FcγRII interact with distinct but overlapping sites on human IgG. J. Immunol. *147*, 2657–2662.

Mallamaci, M.A., Chizzonite, R., Griffin, M., Nettleton, M., Hakimi, J., Tsien, W.H., and Kochan, J.P. (1993). Identification of sites on the human FcεRI alpha subunit which are involved in binding human and rat IgE. J. Biol. Chem. *268*, 22076–22083.

Mao, X.Q., Shirakawa, T., Kawai, M., Enomoto, T., Sasaki, S., Dake, Y., Kitano, H., Hagihara, A., Hopkin, J.M., and Morimoto, K. (1998). Association between asthma and an intragenic variant of CC16 on chromosome 11q13. Clin. Genet. *53*, 54–56.

Maurer, D., Fiebiger, E., Reininger, B., Ebner, C., Petzelbauer, P., Shi, G.P., Chapman, H.A., and Stingl, G. (1998). Fc epsilon receptor I on dendritic cells delivers IgE-bound multivalent antigens into a cathepsin S-dependent pathway of MHC class II presentation. J. Immunol. *161*, 2731–2739.

McDonnell, J.M., Beavil, A.J., Mackay, G.A., Jameson, B.A., Korngold, R., Gould, H.J., and Sutton, B.J. (1996). Structure based design and characterization of peptides that inhibit IgE binding to its high-affinity receptor. Nat. Struct. Biol. *3*, 419–426.

McDonnell, J.M., Beavil, A.J., Mackay, G.A., Henry, A.J., Cook, J.P., Gould, H.J., and Sutton, B.J. (1997). Structure-based design of peptides that inhibit IgE binding to its high-affinity receptor FcεRI. Biochem. Soc. Trans. *25*, 387–392.

Merritt, E.A., and Bacon, D.J. (1997). Raster3D—photorealistic molecular graphics. Methods Enzymol. *277*, 505–524.

Metzger, H. (1992). The receptor with high affinity for IgE. Immunol. Rev. *125*, 37–48.

Metzger, H. (1994). Immunoglobulin receptors. Handicapping the immune response. Curr. Biol. *4*, 644–646.

Miller, K.L., Duchemin, A.M., and Anderson, C.L. (1996). A novel role for the Fc receptor gamma subunit: enhancement of FcγR ligand affinity. J. Exp. Med. *183*, 2227–2233.

Nicholls, A., Sharp, K.A., and Honig, B. (1991). Protein folding and association: insights from the interfacial and thermodynamic properties of hydrocarbons. Proteins *11*, 281–296.

Nissim, A., Jouvin, M.H., and Eshhar, Z. (1991). Mapping of the high affinity Fc epsilon receptor binding site to the third constant region domain of IgE. EMBO J. *10*, 101–107.

O'Reilly, D.R., Miller, L.K., and Luckow, V.A. (1994). Baculovirus Expression Vectors: A Laboratory Manual (Oxford, England: Oxford University Press).

Oettgen, H.C., Martin, T.R., Wynshaw-Boris, A., Deng, C., Drazen, J.M., and Leder, P. (1994). Active anaphylaxis in IgE-deficient mice. Nature *370*, 367–370.

Otwinowski, Z., and Minor, W. (1997). Processing of X-ray diffraction data collected in oscillation mode. In Methods in Enzymology, Volume 276: Macromolecular Crystallography, part A. C.W. Carter and R.M. Sweet, eds. (New York: Academic Press), pp. 307–326.

Presta, L., Shields, R., O'Connell, L., Lahr, S., Porter, J., Gorman, C., and Jardieu, P. (1994). The binding site on human immunoglobulin E for its high affinity receptor. J. Biol. Chem. *269*, 26368–26373.

Ravetch, J.V. (1994). Fc receptors: rubor redux. Cell *78*, 553–560.

Ravetch, J.V., and Clynes, R.A. (1998). Divergent roles for Fc receptors and complement in vivo. Annu. Rev. Immunol. *16*, 421–432.

Ravetch, J.V., and Kinet, J.P. (1991). Fc receptors. Annu. Rev. Immunol. *9*, 457–492.

Robertson, M.W. (1993). Phage and Escherichia coli expression of the human high affinity immunoglobulin E receptor alpha-subunit ectodomain. Domain localization of the IgE-binding site. J. Biol. Chem. *268*, 12736–12743.

Scarselli, E., Esposito, G., and Traboni, C. (1993). Receptor phage. Display of functional domains of the human high affinity IgE receptor on the M13 phage surface. FEBS Lett. *329*, 223–226.

Sechi, S., Roller, P.P., Willette-Brown, J., and Kinet, J.P. (1996). A conformational rearrangement upon binding of IgE to its high affinity receptor. J. Biol. Chem. *271*, 19256–19263.

Shirakawa, T., Li, A., Dubowitz, M., Dekker, J.W., Shaw, A.E., Faux, J.A., Ra, C., Cookson, W.O., and Hopkin, J.M. (1994). Association between atopy and variants of the beta subunit of the high-affinity immunoglobulin E receptor. Nat. Genet. *7*, 125–129.

Su, X.D., Gastinel, L.N., Vaughn, D.E., Faye, I., Poon, P., and Bjorkman, P.J. (1998). Crystal structure of hemolin: a horseshoe shape with implications for homophilic adhesion. Science *281*, 991–995.

Sutton, B.J., and Gould, H.J. (1993). The human IgE network. Nature *366*, 421–428.

Syed, R.S., Reid, S.W., Li, C., Cheetham, J.C., Aoki, K.H., Liu, B., Zhan, H., Osslund, T.D., Chirino, A.J., Zhang, J., et al. (1998). Efficiency of signaling through cytokine receptors depends critically on receptor orientation. Nature *395*, 511–516.

Vigers, G.P., Anderson, L.J., Caffes, P., and Brandhuber, B.J. (1997). Crystal structure of the type-I interleukin-1 receptor complexed with interleukin-1β. Nature *386*, 190–194.